

# Preparation of Fluoroadamantane Acids and Amines: Impact of Bridgehead Fluorine Substitution on the Solution- and Solid-State Properties of Functionalized Adamantanes

V. John Jasy,<sup>†</sup> Franco Lombardo,<sup>†</sup> Troy A. Appleton,<sup>†</sup> Jon Bordner,<sup>†</sup> Martine Ziliox,<sup>‡</sup> and Robert A. Volkmann<sup>\*,†</sup>

Contribution from the Department of Medicinal Chemistry and Neuroscience, Pfizer Central Research, Groton, Connecticut 06340, and Bruker Instruments, Inc., Billerica, Massachusetts 01821

Received July 26, 1999

**Abstract:** Functionalized adamantanes are utilized as medicinal therapeutics and a practical route to novel bridgehead fluorinated adamantylamines and acids including fully fluorinated 3,5,7-trifluoroadamantane-1-carboxylic acid **1** and 3,5,7-trifluoroadamantane-1-amine **2** is described. Potassium permanganate-mediated bridgehead hydroxylation followed by DAST fluorination was utilized to sequentially insert bridgehead fluorine atoms. <sup>13</sup>C NMR chemical shifts of mono-, di-, and trifluoroadamantylamines, acids and carbamates reveal long-range fluorine-mediated electronic effects within the adamantane framework, most notably by substrates bearing three bridgehead fluorine atoms. The impact of multiple bridgehead fluorine substitution on structure (X-ray crystallography) and on physicochemical parameters such as acidity (pK<sub>a</sub>) and lipophilicity (log P) which are important for the design of medicinal therapeutics is assessed.

## Introduction

For over sixty years, adamantane ring-containing compounds have interested organic chemists.<sup>1</sup> The rigid tricyclodecane skeleton has provided a unique structural template for evaluating important theoretical concepts in chemistry. Adamantanes have been particularly useful for probing through-bond and through-space electronic effects<sup>2</sup> and have significantly contributed to our understanding of hyperconjugation (homo-hyperconjugation),<sup>3</sup> and degenerate rearrangements.<sup>4</sup> Furthermore they provide molecular scaffolds for investigating the transmission of electronic effects of remote substituents in saturated systems and its contribution to chemical reactivity<sup>5</sup> and to diastereoselectivity in addition/elimination reactions.<sup>3</sup>

The physical and chemical properties of the adamantane nucleus have largely overshadowed the structure's contribution to the discovery of human therapeutics. Adamantadine<sup>6</sup> (1-aminoadamantane), for example, is currently utilized for the treatment of Parkinson's disease and for the prophylaxis of

influenza infection. Adamantane-containing drugs have shown efficacy as antiviral, hypoglycemic, antiarrhythmic, antidepressant, and antitumor agents, and a number of these compounds are currently in development.<sup>7</sup> Incorporation of the cage-shaped adamantane nucleus into medicinal agents has provided a viable approach for designing molecules which can access lipophilic cell membranes, and this strategy has been particularly useful in facilitating the penetration of the blood–brain barrier by CNS therapeutics.<sup>8</sup>

The benefits of adamantane lipophilicity, however, are often undermined by functionality's susceptibility to metabolic oxidative degradation. P-450 hydroxylation of adamantanes is well documented, with bridgehead oxidation being preferred (3° > 2°).<sup>9</sup> The utility of adamantanes in medicinal chemistry has understandably been hampered by this metabolic liability, and a strategy which exploits the attractive physicochemical and pharmacological properties of adamantanes yet manages to obviate the group's susceptibility to oxidative degradation is greatly needed. Isosteric replacement of the three bridgehead hydrogen atoms with fluorine atoms would provide one such strategy by removing the molecule's major avenue of metabolic degradation while at the same time maintaining the group's overall structure. Fluorine incorporation, however, would likely

\* To whom correspondence should be addressed.

<sup>†</sup> Pfizer Central Research.

<sup>‡</sup> Bruker Instruments, Inc.

(1) (a) Landa, S. *Chem. Listy* **1933**, 27, 415 and **1933**, 27, 443. (b) Fort, R. C., Jr.; von R Schleyer, P. *Chem. Rev.* **1964**, 277–300 and references therein.

(2) (a) Adcock, W.; Kok, G. B. *J. Org. Chem.* **1987**, 52, 356–364. (b) Duddeck, H. *Tetrahedron* **1978**, 34, 247–251. (c) Duddeck, H.; Feuerhelm, H.-T. *ibid.* **1980**, 36, 3009–3015. (d) Duddeck, H.; Hollowood, F.; Karim, A.; McKervey, M. A. *J. Chem. Soc., Perkin Trans. 2* **1979**, 360–365.

(3) (a) Kasej, M.; Adcock, J. L.; Luo, H.; Zhang, H.; Li, H.; le Noble, W. J. *J. Am. Chem. Soc.* **1995**, 117, 7088–7091. (b) Lau, J.; Gonikberg, E. M.; Hung, J.-t.; le Noble, W. J. *ibid.* **1995**, 117, 11421–11425. (c) Adcock, W.; Trout, N. A. *Chem. Rev.* **1999**, 99, 1415–1435.

(4) Majerski, Z.; Liggero, S. H.; von R. Schleyer, P.; Wolf, A. P. *Chem. Commun.* **1970**, 1596–1597.

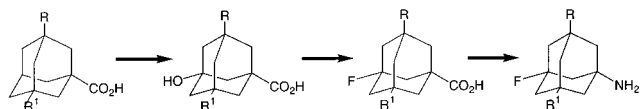
(5) Gleicher, G. J.; von R Schleyer, P. *J. Am. Chem. Soc.* **1967**, 89, 582–593.

(6) (a) Kolocouris, N.; Kolocouris, A.; Foscolos, G. B.; Fytas, G.; Neyts, J.; Padalko, E.; Balzarini, J.; Snoeck, R.; Andrei, G.; De Clercq, E. *J. Med. Chem.* **1996**, 39, 3307–3318. (b) Mueller, R.; Auterhoff, H. *Arch. Pharm.* **1969**, 39, 1–6.

(7) A number of adamantane-containing compounds are commercial drugs or are in clinical development. These include: adapalene (antiacne; multiple sclerosis) Eur. Pat. 199,636, 1989; amantol (antifungal; antibacterial) U.S. Patent 4,288,609, 1981; memantine (peripheral neuropathy; pain; ocular disease) Eur. Pat. 392,059, 1993; rimantadine (influenza, viral infections) U.S. Patent 3,352,912, 1967; tromantadine (antiviral) DE 1,941,218, 1972; SR-48692 (anticancer, neuroleptic) Eur. Pat. 699,438, 1996; HT-90B (antidepressant) WO 93/08182, 1993.

(8) (a) Tsuzuki, N.; Hama, T.; Kawada, M.; Hasui, A.; Konishi, R.; Shiwa, S.; Ochi, Y.; Futaki, S.; Kitagawa, K. *J. Pharm. Sci.* **1994**, 83, 481–484. (b) Tsuzuki, N.; Hama, T.; Hibi, T.; Konishi, R.; Futaki, S.; Kitagawa, K. *Biochem. Pharmacol.* **1991**, 41, R5–R8. (c) Wishnok, J. S. *J. Chem. Educ.* **1973**, 50, 780–781.

(9) (a) White, R. E.; McCarthy, M.-B.; Egeberg, K. D.; Sligar, S. G. *Arch. Biochem. Biophys.* **1984**, 228, 493–502. (b) Raag, R.; Poulos, T. L. *Biochemistry* **1991**, 30, 2674–2684.

**Scheme 1.** General Route to Fluoroadamantanes

effect substrate lipophilicity and, as a result, alter the physico-chemical and pharmacological properties of the adamantane core. The magnitude of such an effect is unknown and certainly would be an important determinant for the utility of these substrates in drug discovery.

Since a number of important adamantane-containing drugs can be generated from adamantane-1-carboxylic acid or adamantane-1-amine, fluorine-substituted derivatives of these two key synthons were selected as synthetic targets for testing the viability of this overall approach. In addition to possible medicinal applications, these substrates would likely also be of interest for assessing bridgehead fluorine-mediated through-bond and through-space electronic effects, given the structural rigidity of the adamantane nucleus. Accordingly, we describe herein the preparation of bridgehead-bearing fluorine-substituted adamantane amines and acids including 3,5,7-trifluoroadamantane-1-carboxylic acid **1** and 3,5,7-trifluoroadamantane-1-amine **2** and the selected physical properties of these compounds.

## Results and Discussion

**Fluoroadamantane Synthesis.** Three synthetic strategies were entertained for bridgehead fluorine incorporation: (1) direct adamantane fluorination,<sup>10</sup> (2) halogen (bromine/chlorine/iodine) insertion followed by fluorine exchange,<sup>11</sup> and (3) sequential bridgehead oxidation—alcohol-to-fluorine conversion.<sup>12</sup> We opted for the latter since the technology for monohydroxylation of bridgehead carbon atoms is well established, as is the conversion of tertiary alcohols to fluorides. While the ability to hydroxylate mono- and difluoroadamantane carboxylic acids had not been previously demonstrated, the likelihood for sequential application of this method seemed reasonable, thereby providing a potential route to di- and trisubstituted fluoroadamantane acids. These acids, in turn, would be logical precursors (via Curtius rearrangement) to the corresponding substituted fluoroadamantylamines. This somewhat lengthy protocol (Scheme 1) would allow the entire set of mono-, di-, and trifluoro bridgehead adamantylamines (and carbamates) and acids to be generated, thereby providing interesting medicinal synthons as well as structures of potential theoretical interest, capable of probing fluorine-mediated through-bond and through-space electronic effects on the rigid saturated adamantane acid and amine core.

The starting 3-fluoroadamantane carboxylic acid **3**,<sup>2a,13</sup> mp 154–156 °C, was easily obtained from 3-hydroxyadamantane carboxylic acid. This transformation along with the direct conversion of **3** to 3-fluoroadamantane-1-amine **5**,<sup>2a,13d,14a</sup> have been previously described.<sup>2a,13d</sup> We opted, in addition, to isolate

carbamate **4** as well as di- and trifluoroadamantane carbamates in the course of this work. Accordingly, **3** was treated with diphenylphosphoryl azide<sup>15</sup> (TEA, benzyl alcohol 70 °C) to afford benzyl carbamate **4**. Hydrogenolysis (10% Pd/C, HOAc) cleanly yielded amine **5** as its acetate salt (Figure 1).

Oxidation of mono- and difluoroadamantane carboxylic acids would be required to access the remaining alcohol targets, and their preparation suggested a number of viable reagents. Dimethyldioxirane,<sup>16</sup> potassium permanganate,<sup>13d</sup> ferrous iron—molecular oxygen,<sup>17</sup> and perfluorooxaziridines<sup>18</sup> have been utilized to generate 3-hydroxy-1-adamantanecarboxylic acid from adamantane carboxylic acid. Treatment of the sodium salt of 3-fluoroadamantane carboxylic acid **3** with potassium permanganate afforded, after removal of unreacted starting material and esterification (methyl iodide treatment of the product's tetrabutylammonium salt), methyl-3-fluoro-5-hydroxyadamantane-1-carboxylate **6**.

Diethylaminosulfur trifluoride (DAST)-mediated fluorinations of alcohols have been utilized for generating, in high yield, a variety of fluorides, and this reagent was a logical choice for accessing the desired bridgehead fluorides.<sup>12</sup> Treatment of **6** with DAST in refluxing chloroform followed by saponification of the crude product afforded 3,5-difluoroadamantane-1-carboxylic acid **7**,<sup>19</sup> mp 162–164 °C, in >95% yield. 3,5-Difluoroadamantane-1-amine **9** could be smoothly obtained, as described for the conversion of **3** to **5**, as its acetate salt by treatment of **7** with diphenylphosphoryl azide (TEA, benzyl alcohol 70 °C) and subsequent hydrogenolysis of the resultant benzyl carbamate **8** (10% Pd/C, HOAc).

The same protocol employed for the synthesis of 3,5-difluoroadamantane-1-carboxylic acid **7** and amine **9** was adapted for the preparation of the trifluoroadamantane analogues. Both the potassium permanganate oxidation to generate **10** and the resultant DAST fluorination required higher temperatures/longer reaction times, reflecting the presence of the additional electron-withdrawing fluorine substituents. Nonetheless, 3,5,7-trifluoroadamantane-1-carboxylic acid **1**, mp 198–199 °C, carbamate **11**, mp 91.5–92.0 °C, and amine **2** as its acetate salt were generated using this procedure.

**Spectroscopic Data.** <sup>13</sup>C and <sup>19</sup>F NMR spectroscopy has been utilized to probe the through-bond and through-space electronic effects of substituents in structurally rigid organic substrates and to quantify polar substituent effects in saturated systems. Substituted fluoroadamantanes including 3-substituted-1-fluoroadamantanes,<sup>2a,20</sup> perfluoroadamantyl halides,<sup>21</sup> fluorodiadamantanes,<sup>11a</sup> mono-, di-, tri-, and tetrafluoroadamantanes<sup>2a,11a</sup> were examined in these pioneering studies, and these data, in concert with reaction rate (solvolyses) and/or equilibria data, have revealed a rather complicated picture of electronic transmission modes in saturated systems. Long-range adamantyl substituent effects have been examined by <sup>13</sup>C NMR. While definite trends are revealed for proximal and distal methylene carbon resonances, bridgehead carbon resonances have proven less predictable.<sup>11a</sup>

(10) Gal, C.; Rozen, S. *Tetrahedron Lett.* **1985**, *26*, 2793–2796.

(11) (a) Olah, G. A.; Shih, J. G.; Krishnamurthy, V. V.; Singh, B. P. *J. Am. Chem. Soc.* **1984**, *106*, 4492–4500. (b) Bhandari, K. S.; Pincock, R. E. *Synthesis* **1974**, 655–656.

(12) Middleton, W. J. *J. Org. Chem.* **1975**, *40*, 574–578.

(13) (a) Stetter, H.; Mayer, J. *Chem. Ber.* **1962**, *95*, 667–672. (b) Bolte, G.; Haas, A. *ibid.* **1984**, *117*, 1982–1986. (c) Bolte, G.; Haas, A. *J. Fluorine Chem.* **1983**, *23*, 502. (d) Anderson, G. L.; Burks, W. A.; Harruna, I. I. *Synth. Commun.* **1988**, *18*, 1967–1974.

(14) (a) Kollonitsch, J.; Barash, L.; Doldouras, G. A. *J. Am. Chem. Soc.* **1970**, *92*, 7494–7495. (b) Anderson, G. L.; Randolph, B. J.; Harruna, I. I. *Synth. Commun.* **1989**, *19*, 1955–1963.

(15) Huc, I.; Rebeck, J., Jr. *Tetrahedron Lett.* **1994**, *35*, 1035–1038.

(16) Murray, R. W.; Gu, H. *J. Org. Chem.* **1995**, *60*, 5673–5677.

(17) Miura, T.; Shibata, K.; Sawaya, T.; Kimura, M. *Chem. Pharm. Bull.* **1982**, *30*, 67–73.

(18) Sorochinsky, A. E.; Petrenko, A. A.; Soloshonok, V. A.; Resnati, G. *Tetrahedron* **1997**, *53*, 5995–6000.

(19) Sorochinsky, A. E.; Aleksandrov, A. M.; Kukhar, V. P.; Gamaleya, V. F.; Krasnoshechek, A. P. *J. Org. Chem. USSR (Engl. Transl.)* **1979**, *15*, 2240–2244.

(20) Wahl, G. H., Jr.; Peterson, M. R., Jr. *J. Am. Chem. Soc.* **1970**, *92*, 7238–7239.

(21) Adcock, J. L.; Luo, H.; Dai, S. *Magn. Reson. Chem.* **1993**, *31*, 969–971.

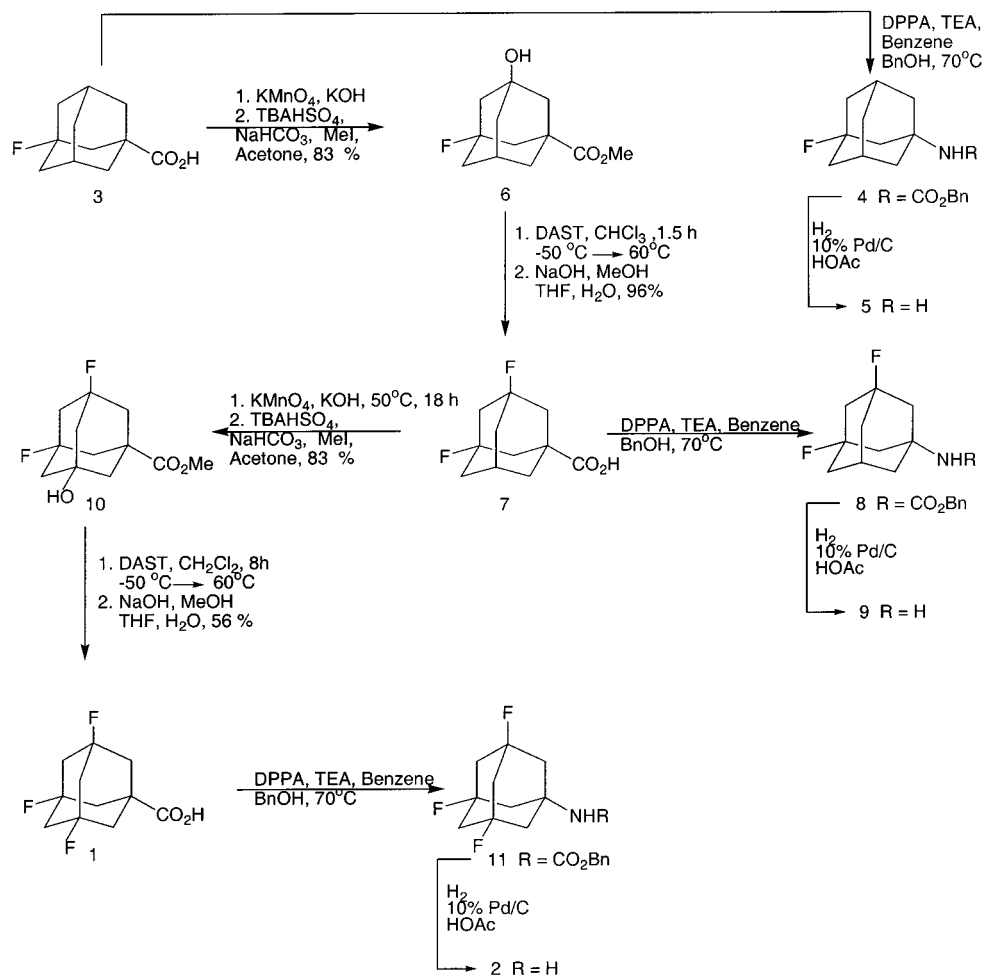


**Figure 1.** Fluoroadamantane acid/amine synthesis.

$^{13}\text{C}$  NMR chemical shifts were obtained for fluoroadamantyl carbamates **4**, **8**, and **11**, amines **2**, **5**, and **9** and acids **1**, **3**, and **7** and are shown in Table 1. Comparative analysis of  $^{13}\text{C}$  NMR chemical shifts for the fluoroadamantanes reveal interesting effects resulting from bridgehead fluorine substitution, particularly at the bridgehead carbon atoms. A downfield shift in the  $^{13}\text{C}$  NMR was observed for the bridgehead carbon atoms bearing acid, amine, and carbamate groups with sequential addition of up to two bridgehead fluorine atoms (carbon 1, Table 1), consistent with removal of electron density at this center. Replacement of the last remaining bridgehead hydrogen atom to generate the trifluoroadamantyl derivatives **1**, **2**, and **11**, however, results, in all three cases, in an *upfield*  $^{13}\text{C}$  NMR chemical shift at this center (greater than 2 ppm higher than the corresponding difluoro derivatives). In addition, similar results were obtained for the fluorine-bearing bridgehead carbon atoms (carbon atom 3, Table 1) as an *upfield* shift (1.2–2.0 ppm) was observed for the fluorine-bearing bridgehead carbon atoms in trifluoroadamantyl derivatives **1**, **2**, and **11**.

Selected  $^{13}\text{C}$ – $^{19}\text{F}$  coupling constants are included in Table 1. Sequential addition of bridgehead fluorine atoms results in an increase in carbon–fluorine coupling. For example, in the carbamate series,  $^1J_{\text{C}_3\text{F}}$  (trifluoroadamantane **11**) = 190.29 >  $^1J_{\text{C}_3\text{F}}$  (difluoroadamantane **8**) = 188.67 >  $^1J_{\text{C}_3\text{F}}$  (monofluoroadamantane **4**) = 184.30. A similar trend was obtained in the amine and acid series. Also sequential addition of fluorine atoms on the adamantane framework provides a progressive increase in  $^{19}\text{F}$  NMR chemical shifts. For example, the  $^{19}\text{F}$  NMR chemical shift for monofluoroadamantane amine salt **5** was

–129.14 ppm while difluoroadamantane **9** was –135.78 ppm and trifluoroadamantane **2** was at –144.33 ppm.

**X-ray Crystallographic Data.** Considering the rigid adamantane template, small molecular distortions in the solid-state structures of mono-, di-, and trifluoroadamantane derivatives could serve as an indicator of significant inductive, electronic, and polarization effects caused by the fluorine-containing bridgehead carbon atoms. While symmetrically substituted adamantanes often do not form crystals suitable for X-ray structural determination due to the formation of plastic crystalline phases,<sup>22</sup> the fact that adamantane-1,3,5,7-tetracarboxylic acid<sup>23</sup> as well as bridgehead halogenated adamantanes<sup>24</sup> have been crystallized was encouraging.

X-ray structures were obtained for mono-, di-, and trifluoroadamantane carboxylic acids **3**, **7**, and **1**. Similar to adamantane carboxylic acid,<sup>25</sup> di- and trifluoroadamantane acids **7** and **1** crystallize as two molecules in the asymmetric unit joined together by hydrogen bonding of the carboxylic acid moiety. Selected adamantane bond lengths and angles are shown in Figures 2 and 3. A complete summary of bond angles and bond lengths of these compounds is included with the Supporting

(22) a) Fort, R. C., Jr. *Adamantane. The Chemistry of Diamond Molecules*; Marcel Dekker: New York, 1976. (b) Rao, C. N. R. In *Organic Solid State Chemistry*; Desiraju, G. R., Ed.; Elsevier: Amsterdam, 1987; p 371.

(23) Ermer, O. *J. Am. Chem. Soc.* **1988**, *110*, 3747–3754.

(24) Bremer, M.; Gregory, P. S.; von R Schleyer, P. *J. Org. Chem.* **1989**, *54*, 3796–3799.

(25) Belanger-Gariepy, F.; Brisse, F.; Harvey, P. D.; Gilson, D. F. R.; Butler, I. S. *Can. J. Chem.* **1990**, *68*, 1163–1169.

**Table 1.**  $^{13}\text{C}$  NMR Chemical Shifts of the Fluoroadamantanones<sup>a-d</sup>

	<u>1</u>	<u>2</u>	<u>3</u>	<u>4</u>	<u>5</u>	<u>6</u>	<u>7</u>	<u>8</u>	<u>9</u>	<u>10</u>	<u>11</u>
	53.80 (d) (12.23)	46.57 (d) (18.79)	92.30 (d) (184.30)	40.25	30.80 (d) (10.19)	34.52 (d) (1.81)	30.80 (d) (10.19)	41.48 (d) (17.74)	41.48 (d) (17.74)	40.25	
	54.25 (t)	45.54 (m)	92.24 (dd) (188.67, 14.7)	45.54 (m)	92.24 (dd) (188.67, 14.7)	40.15 (m)	29.07 (t)	40.15 (m)	47.16 (t)	38.98	
	52.08 (q) (14.9)	44.65 (m)	90.69 (dt) (190.29, 16.6)	44.65 (m)	90.69 (dt) (190.29, 16.6)	46.22 (m)	90.69 (dt) (190.29, 16.6)	46.22 (m)	46.22 (m)	44.65 (m)	
	54.43 (d) (12.36)	44.59 (d) (20.77)	93.57 (d) (182.29)  $^{19}\text{F}$ -129.14	38.20 (d) (1.28)	30.35 (d) (10.46)	32.87 (d) (1.81)	30.35 (d) (10.46)	40.00 (d) (17.06)	40.00 (d) (17.06)	38.20 (d) (1.28)	
	54.76 (t)	43.79 (m)	93.38 (dd) (186.8, 15.0)  $^{19}\text{F}$ -135.78	43.79 (m)	93.38 (dd) (186.8, 15.0)  $^{19}\text{F}$ -135.78	38.96 (m)	29.09 (t)	38.96 (m)	45.94 (t)	37.26	
	52.31 (q)	42.82 (m)	91.49 (dt)  $^{19}\text{F}$ -144.33	42.82 (m)	91.49 (dt)  $^{19}\text{F}$ -144.33	44.80 (m)	91.49 (dt)  $^{19}\text{F}$ -144.33	44.80 (m)	44.80 (m)	42.82 (m)	
	44.66 (d) (10.35)	43.32 (d) (20.32)	92.0 (d) (184.15)  $^{19}\text{F}$ -130.02	37.27 (d) (1.56)	30.73 (d) (10.06)	34.67 (d) (1.52)	30.73 (d) (10.06)	41.71 (d) (17.54)	41.71 (d) (17.54)	37.27 (d) (1.56)	182.41
	45.51 (t)	42.41 (m)	92.64 (dd) (188.6, 13.9)  $^{19}\text{F}$ -134.58	42.41 (m)	92.64 (dd) (188.6, 13.9)  $^{19}\text{F}$ -134.58	40.31 (m)	30.50 (t)	40.31 (m)	47.31 (t)	36.18	180.68
	43.03 (q)	41.53 (m)	91.49 (dt) (191.6, 15.4)	41.53 (m)	91.49 (dt) (191.6, 15.4)	46.21 (m)	91.49 (dt) (191.6, 15.4)	46.21 (m)	46.21 (m)	41.53 (m)	179.33

<sup>a</sup> Chemicals shifts are in ppm ( $\pm 0.05$ ) with respect to external  $\text{Me}_4\text{Si}$  in  $\text{CDCl}_3$  at 20 °C. <sup>b</sup> d = double, t = triplet, q = quartet, m = complex multiplet, dd = double of doublets, dt = doublet of triplets—these refer to C–F coupling patterns. <sup>c</sup>  $^{13}\text{C}$ – $^{19}\text{F}$  coupling constants (in hertz) are given in parentheses. <sup>d</sup>  $^{19}\text{F}$  chemical shifts are in ppm ( $\pm 0.05$ ) with respect to external  $\text{CFCl}_3$  in  $\text{CDCl}_3$  at 20 °C. Negative sign indicates upfield shift.

Information. The bridgehead fluorine atom(s) not only influence the crystal packing within the unit cell but also bond lengths (and angles) within the adamantane skeleton. Bond lengths of mono- and difluoroadamantane acids **3** and **7** are well ordered. Given the pseudoplane of symmetry (neglecting the acid torsional angle) in monofluoroadamantane **3** (plane through C-1, C-3, and C-6) and difluoroadamantane **7** (plane through C-1,

C-7, and C-9), bond lengths reflect the symmetry of the adamantane skeleton, and equivalent adamantyl carbon–carbon bonds vary by  $< 0.02$  Å.

In contrast, the X-ray crystal structure of trifluoroadamantane acid **1** reveals a disordered structure that crystallizes as two distinct (and not equivalent) entities, with C–C adamantyl bond lengths ranging from 1.438 to 1.595 Å (Figure 2) and bond



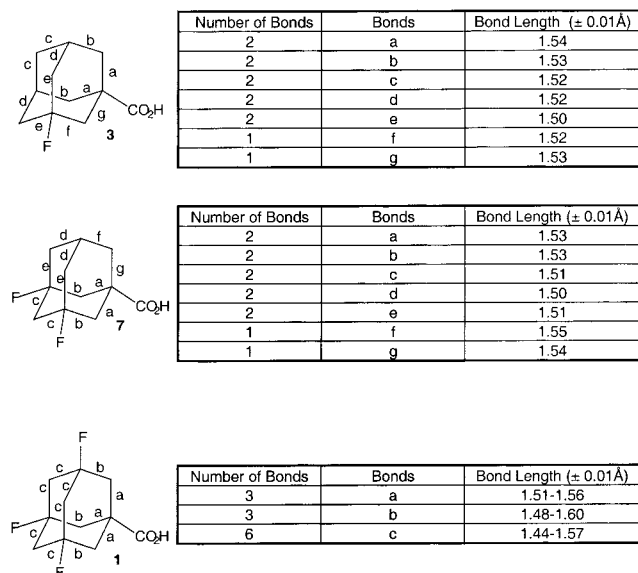


**Figure 2.** Carbon-carbon bond lengths of fluoroadamantanes **3**, **7** and **1** were obtained from the X-ray crystallographic data. Di- and trifluoroadamantane carboxylic acids have two molecules in the asymmetric unit and bond lengths from both molecules are included.

Adamantane Carboxylic Acid	Average Internal Adamantane C-C-C Bond Angle: Acid Bearing Carbon 1	Average Internal Adamantane C-C-C Bond Angle: Fluorine Bearing Carbon 3 (5 & 7 when applicable)	Average External Adamantane C-C-CO <sub>2</sub> H Bond Angle: Acid Bearing Carbon 1	Average External Adamantane C-C-F Bond Angle: Fluorine Bearing Carbon 3 (5 & 7 when applicable)
Monofluoro <b>3</b>	108.8	110.9	110.1	108.0
Difluoro <b>7</b>	108.8	110.5	110.1	108.4
Trifluoro <b>1</b>	109.8	110.8	109.2	108.0

**Figure 3.** Selected C-C-C and C-C-F bond angles of fluoroadamantanes **3**, **7**, and **1** were obtained from the X-ray crystallographic data. Adamantane carbon atoms are labeled as shown in Table 1.

angles ranging from 104.5° to 114.1°. That the X-ray crystal structure of trifluoroadamantane acid **1** is an aberration appears not to be the case. X-ray crystal structures of adamantane-1-carboxylic acid<sup>25</sup> (bearing three bridgehead hydrogen atoms) and 1,3,5 trifluoro-7-iodoadamantane<sup>24</sup> show similar distortion of the adamantane framework at ambient temperature. Moreover, X-ray studies have shown that a number of adamantane-containing compounds such as 1- and 2-hydroxyadamantane, 1-adamantanamine, 1-halogenoadamantanes, and a number of alkyladamantanes undergo an order-disorder transition, and the effect of substituent groups on the disordered phase behavior of these molecules has been investigated.<sup>26</sup> The crystal structure of adamantane-1-carboxylic acid has been determined by X-ray diffraction at two temperatures, 173 and 280 K. At both temperatures, the unit cells are triclinic, space group *P1*, and each contains two molecules. The low-temperature form is ordered, while the molecule at room temperature is disordered.<sup>25</sup>

**Solid State <sup>13</sup>C NMR.** Since solution NMR data was utilized to assess the long-range electronic effects exerted by the adamantane bridgehead fluorine substituents and the structural data for the three fluoroadamantane acids resides with single-crystal X-ray crystallographic analyses, solid state <sup>13</sup>C NMR spectra (13 kHz) using regular CP-MAS were obtained for mono-, di-, and trifluoroadamantane acids **3**, **7**, and **1** to complement the solution data. Not all of the carbon atoms in the solid state spectra were definitively assigned. Nonetheless, by utilizing dipolar dephasing to suppress carbon atoms with strong dipolar coupling to protons, those not directly attached

#### Effect of Bridgehead Fluorine Substitution on Acidity and Lipophilicity of Adamantane Carboxylic Acids and Amines

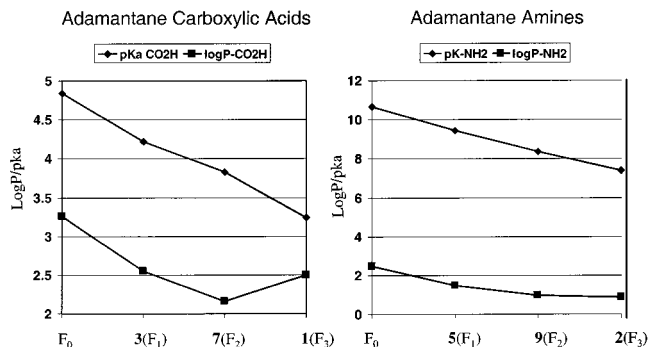


**Figure 4.** The aqueous  $pK_a$ 's were determined by potentiometric titration. Log  $P$  values were determined by potentiometric methods by comparing the aqueous  $pK_a$ 's to those obtained with octanol. Compound assignments are in bold. The subscripts in  $F_0$ ,  $F_1$ ,  $F_2$ ,  $F_3$  refer to the number of adamantane bridgehead fluorine atoms.

to hydrogen (i.e., the carboxyl-bearing bridgehead carbon atom) could be assigned. The solid state <sup>13</sup>C NMR spectra supported the X-ray crystallography data as doubling of resonances were observed, consistent with inequivalent sites in the crystal structure. Particularly noteworthy was the chemical shift of the bridgehead carbon atom bearing the carboxylic acid moiety. The bridgehead carbon atom for monofluoro **3** was found at 45.705 and 45.963 ppm and difluoro **7** at 46.629 ppm, displaying the same trend seen in solution NMR. Once again, a significant upfield shift (43.968 and 41.930 ppm) was observed for the carboxyl-bearing bridgehead carbon atom in both molecules of trifluoroadamantane acid **1** found in the asymmetric unit, demonstrating that the solid-state NMR data mirrors that of solution NMR, and both, in concert with the X-ray crystallography data, are appropriate for assessing the electronic and structural effects of bridgehead fluorine substitution.

**Physicochemical Parameters of Fluoroadamantanes.** The impact of long-range electronic and structural effects resulting from fluorine substitution on physicochemical parameters such as acidity ( $pK_a$ ) and lipophilicity ( $\log P_{\text{oct}}$ ), which are important for the design of medicinal therapeutics, is open to question.  $\log P_{\text{oct}}$  and  $pK_a$  values for the adamantane acids and amines were obtained by potentiometric titration<sup>27</sup> as described in the Experimental Section. Substrates in aqueous 0.167 M NaCl at low pH were titrated with 0.5 N NaOH to determine the  $pK_a$ 's. The solutions were reacidified, treated with 1-octanol and titrated again.  $\log P_{\text{oct}}$  values were calculated from shifts in the  $pK_a$  titration curves obtained with 1-octanol.

Typically, sequential addition of fluorine atoms to aliphatic molecules results in incremental changes in both  $pK_a$  and  $\log P_{\text{oct}}$  values.<sup>28</sup> Bridgehead fluorine incorporation has a significant impact on the acidity of the adamantane acids. A linear relationship exists between fluorine substitution and  $pK_a$  (Figure 4). Accordingly, trifluoroadamantane carboxylic acid **1** has a  $pK_a$  value of  $3.24 \pm 0.07$ , while difluoroadamantane acid **7** has a value of  $3.83 \pm 0.04$  and monofluoro **3** a value of  $4.22 \pm 0.02$ . This relationship follows suit with the corresponding adamantylamines with the conjugate acid of trifluoroadamantane amine **2** having a  $pK_a$  value of  $7.39 \pm 0.02$  (versus  $8.36 \pm 0.02$  for difluoro **9** and  $9.45 \pm 0.02$  for monofluoro **5**).

(27) (a) Avdeef, D. *J. Pharm. Sci.* **1993**, *82*, 183-190. (b) Avdeef, A.; Barrett, D. A.; Shaw, P. N.; Knaggs, R. D.; Davis, S. S. *J. Med. Chem.* **1996**, *39*, 4377-4381.

(28) Chambers, R. D. In *Interscience Monographs in Organic Chemistry: Fluorine in Organic Chemistry*; John Wiley and Sons: New York, 1973.

(26) Clark, T.; Mc. O. T.; Knox, H.; Mackle, H.; McKervey, M. A. *J. Chem. Soc., Faraday Trans. 1* **1977**, *73*, 1224-1231.

While fluorine addition to aromatic rings generally increases substrate lipophilicity, addition to saturated aliphatic compounds results in a decrease in lipophilicity as measured by  $\log P_{\text{oct}}$ . In the case of the fluoroadamantanes, the relationship between extent of fluorine substitution and substrate lipophilicity ( $\log P_{\text{oct}}$ )<sup>27</sup> is not linear and diverges once three bridgehead fluorine atoms have been added to the adamantane framework. Fluorine incorporation results in a decrease in substrate lipophilicity for mono ( $\log P_{\text{oct}} 2.55 \pm 0.04$ ) and difluoro ( $\log P_{\text{oct}} 2.16 \pm 0.08$ ) acids **3** and **7** versus adamantane carboxylic acid ( $\log P_{\text{oct}} 3.26 \pm 0.04$ ) and mono- ( $\log P_{\text{oct}} 1.48 \pm 0.04$ ) and difluoro ( $\log P_{\text{oct}} 0.98 \pm 0.10$ ) amines **5** and **9** versus adamantylamine ( $\log P_{\text{oct}} 2.47 \pm 0.04$ ). The decrease in  $\log P_{\text{oct}}$  value for trifluoro-adamantane amine **2** ( $\log P_{\text{oct}} 0.88 \pm 0.06$ ), however, is smaller than anticipated, and in fact an *increase* in  $\log P_{\text{oct}}$  (2.50  $\pm$  0.14) is observed for trifluoroadamantane carboxylic acid **1** (Figure 4).

## Discussion

X-ray crystallographic data for adamantane acids **3**, **7**, and **1** in concert with <sup>13</sup>C NMR analysis of the nine adamantane acids, amines, and carbamates reveal significant structural and electronic effects mediated by the bridgehead fluorine atoms present in these molecules. The reason behind the unexpected upfield <sup>13</sup>C NMR chemical shift for the bridgehead carbon atom bearing acid, amine, and carbamate groups upon addition of a third fluorine atom is subject to debate. It is tempting to correlate the <sup>13</sup>C NMR shifts with the internal C–C–C bond angles obtained from the X-ray crystallographic data. The addition of bridgehead fluorine atoms would be expected to effect carbon hybridization since the electronegative fluorine atom should pull p character into the C–F bond, thereby increasing the s character of the C–C bonds at these centers. In addition to through-bond and through-space inductive effects, one would expect that, as the internal adamantane C–C–C bond angles at these centers get larger, the <sup>13</sup>C NMR chemical shifts should increase (downfield shift) because there is more s character in the C–C bonds.

The X-ray crystallographic data of adamantane acids **3**, **7**, and **1** indicate that, at the fluorine-substituted bridgehead carbon atoms, the average external C–C–F bond angles are less than 109.5° and the internal C–C–C bonds greater than 109.5° (Figure 3). In the case of monofluoroadamantane carboxylic acid **3**, for example, the average external C–C–F bond angle is 108.0°, while the average internal C–C–C bond angle at this center is 110.9°. In the case of difluoroadamantane carboxylic acid **7**, the average external C–C–F bond angle value is 108.4°, while the average internal C–C–C value at the two centers is 110.5°. The situation is just the opposite for the carboxyl-bearing bridgehead carbon atom where the average value for external C–C–COOH bond angles for monofluoro-adamantane acid **3** and difluoroadamantane acid **7** is 110.1°, while the average value for internal C–C–C bond angles is 108.8° for **3** and **7**. One would assume that trifluoroadamantane acid **1** would have three large internal C–C–C bond angles at the fluorine-bearing carbon atoms, leading to a further decrease in the internal C–C–C bond angle at the carboxyl-bearing center. The net result would be an upfield shift in the <sup>13</sup>C NMR for this bridgehead carbon atom. Because of the distortion of the adamantane nucleus in X-ray crystal of **1**, data analysis is subject to question. However, if one averages bond angles for equivalent carbon atoms, one finds that the average internal C–C–C bond angle for the carboxyl-bearing carbon atom is 109.8° (versus 108.8° for **3** and **7**). Such an increase in the

internal C–C–C bond angle at this center would be expected to provide a *downfield shift*, as opposed to the 2.48 ppm upfield shift which was seen in the <sup>13</sup>C NMR of **1**, **2**, and **11**.

The fact that the lipophilicity of the fluorinated adamantanes shows a nonlinear behavior (Figure 4) was also, at first, puzzling and difficult to rationalize, since the addition of a fluorine atom in going from difluoro **7** to trifluoro acid **1** was not expected to have a great impact on the partition of these species between water and octanol. One explanation that could be given is that the carboxylic acids might self-associate and form a more lipophilic “supramolecular” adduct which might partition more easily into the organic phase, but it seemed unlikely that such a sudden change would take place in going from **7** to **1**. Furthermore, Schweitzer and Morris<sup>29</sup> report that the dimerization (association) constant for octanoic acid in 1-hexanol is essentially zero and Kojima et al.<sup>30</sup> report rather similar findings for propanoic acid, derived from distribution experiments between water and hydrogen-bonding organic solvents.

The linear free-energy relationship (LFER) developed by Abraham<sup>31</sup> for  $\log P_{\text{oct}}$  has been employed to correlate octanol–water partition with solvation parameters such as the hydrogen bond donor and acceptor capability of a given solute. Initially, we sought to confirm, by an independent method, that the order of lipophilicity observed by the reverse titration method was indeed correct. Pagliara et al.<sup>32</sup> have shown that a good correlation between the  $\log P_{\text{oct}}$  and HPLC capacity factors ( $k'$ ) can be observed under specified sets of conditions, and Abraham et al.<sup>33</sup> have also confirmed these observations and expanded the analysis of HPLC stationary and mobile phases to include correlations between  $\log P_{\text{alk}}$  and HPLC  $k'$  values, via their solvation parameters.

The method of Pagliara et al. uses either the  $k'$  at 40% methanol ( $k'_{40}$ ) or extrapolated values ( $k'_w$ ) at 0% of organic solvent, on a Supelcosil LC-ABZ column, to correlate the capacity factors to  $\log P_{\text{oct}}$  values. Even the 40% methanol mobile phase, in our hands, gave very long retention times for the adamantane acids. As a result, we resorted to the extrapolation of  $k'$  from a mobile phase containing 65% of methanol down to 45% methanol, in 5% intervals. Under all of these conditions, trifluoro acid **1** eluted *always* between difluoro and monofluoro acids **3** and **7**, and no crossover was observed. A good linearity was found for the capacity factors of each compound, and the extrapolation to either mobile phase recommended by Pagliara et al. showed that, indeed, the lipophilicity was in the same order as found via the reverse titration method. Incidentally, computed  $\log P_{\text{oct}}$  values for the fluoroadamantane carboxylic acids, obtained from commonly available fragmental constant methods, were not predictive of the observed results.

The LFER equation mentioned above<sup>31</sup> considers several parameters such as the hydrogen-bonding (donor and acceptor) capability, the dipolarity/polarizability, the volume, and the molar refractivity of the solutes. A retrospective analysis of these parameters demonstrated, as expected, that all of the values are either progressively increasing (H-bond acidity, volume) or decreasing (H-bond basicity, excess molar refractivity), and the

(29) Schweitzer, G. K.; Morris, D. K. *Anal. Chim. Acta* **1969**, *45*, 65–70.

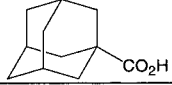
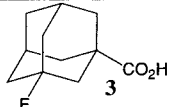
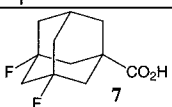
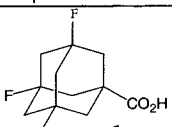
(30) Kojima, I.; Yoshida, M.; Tanaka, M. *J. Inorg. Nucl. Chem.* **1970**, *32*, 987–995.

(31) Abraham, M. H.; Chadha, H. S.; Whiting, G. S.; Mitchell, R. C. *J. Pharm. Sci.* **1994**, *83*, 1085–1100.

(32) Pagliara, A.; Khamis, E.; Trinh, A.; Carrupt, P.-A.; Tsay, R.-S.; Testa, B. *J. Liq. Chromatogr.* **1995**, *18*, 1721–1745.

(33) Abraham, M. H.; Chadha, H. S.; Leitao, R. A. E.; Mitchell, R. C.; Lambert, W. J.; Kalisz, R.; Nasal, A.; Haber, P. *J. Chromatogr. A* **1997**, *766*, 35–47.

**Table 2.** Dipole Moments<sup>a</sup> and Dipolarity/Polarizability<sup>b</sup> Value Calculated for Fluoroadamantanes

Adamantane Carboxylic Acids	MMFF Dipole Moment (D)	AM1 Dipole Moment (D)	HF/6-31G* Dipole Moment (D)	Dipolarity/Polarizability
	1.48	2.12	1.95	1.09
	1.87	1.89	1.86	1.57
	3.21	2.56	3.10	2.02
	2.25	1.16	1.89	1.82

<sup>a</sup> All dipole moment computations were performed using the Spartan software package, version 5.1. All values were generated in the gas phase. MMFF = Merck Molecular Force Field. AM1 = Austin Model 1. See Experimental Section. <sup>b</sup> See refs 33–34.

change is relatively modest, across the series of four adamantane carboxylic acids.<sup>34</sup> In the LFER equation, it turns out, the coefficient for the hydrogen bond basicity is very large, with a value of  $-3.46$ .<sup>31</sup> This factor, a priori, might have influenced the behavior of these analogues, if a larger difference between **7** and **1**, were to be observed in terms of their hydrogen bond basicity. That is, a significant decrease in the value of this parameter, between the two analogues considered, and brought about by the presence of a third fluorine atom would have resulted in a significant contribution toward a higher log *P* value. The estimate for the series of analogues, it was found, called instead for a fairly modest and linear decrease across the series, and the hydrogen bond basicity could not be invoked as an explanation.<sup>34</sup> Dipolarity/polarizability, however, does change significantly across the series and reaches a maximum for difluoro acid **7** and then a decrease is observed for trifluoro acid **1**. This observation, when coupled with the significant negative coefficient found for the dipolarity/polarizability term ( $-1.05$ ) in the Abraham's solvation equation,<sup>33</sup> points to the fact that the observed shift in this parameter is the likely cause of the upward shift in log *P*<sub>oct</sub>. Table 2 shows the values of this parameter for the adamantane carboxylic acids.<sup>34</sup>

We also have computed, at different levels of theory, the dipole moment of the adamantane acids considered in this work, and we found that in all cases there is a maximum reached for **7** and then a significant decrease for **1**, further confirming the fact that the dipole moment change is responsible for the observed shift in log *P*<sub>oct</sub>. Table 2 shows the results of the computations, and a clear shift is observed in going from **7** to **1**.

## Conclusions

In summary, a synthetic route has been developed to access heretofore unknown trifluoroadamantane acid **1** and amine **2** along with related bridgehead-substituted fluoroadamantane acids **3** and **7** and amines **5** and **9**, possible synthons in medicinal chemistry. The influence of bridgehead fluorine substitution on structure (X-ray crystallography) and on physicochemical parameters such as acidity (*pK*<sub>a</sub>) and lipophilicity (log *P*<sub>oct</sub>), which are important for the design of medicinal therapeutics,

is significant. The impact of three bridgehead fluorine atoms is particularly noteworthy. X-ray crystallography reveals a *highly dis-symmetric* structure for trifluoroadamantane acid **1**, which crystallizes as two distinct (and nonequivalent) entities.

<sup>13</sup>C NMR chemical shifts for the bridgehead carbon atoms in the trifluoroadamantylamines, acids, and carbamates are not well understood. Neither simple inductive and polarization factors nor internal C–C–C bond angles account for the <sup>13</sup>C NMR chemical shifts of the bridgehead carbon atoms in these molecules. The NMR data along with the log *P*<sub>oct</sub> values underscore significant through-space effects resulting from the incorporation of three bridgehead fluorine atoms in the adamantane framework. An increase in log *P*<sub>oct</sub> resulting from the incorporation of a third fluorine atom in the adamantane framework was not expected, but parallels predicted differences in the dipole moments of the fluoroadamantane acids.

## Methods

**Apparatus.** The computerized titration instrument (Sirius PCA 101) was used by Water Technology Associates to perform the *pK*<sub>a</sub> and log *P* assays, which have been previously described in detail.<sup>27</sup>

**Potentiometric Titrations.** The aqueous *pK*<sub>a</sub> was determined by potentiometric titration. If compounds were water insoluble, apparent *pK*<sub>a</sub>'s were found in water/solvent ratios and the aqueous *pK*<sub>a</sub> was found by extrapolating to 0% solvent according to the Yasuda–Shedlovsky technique.<sup>35</sup> The pH-metric technique consisted of two linked titrations. The first titration is carried out in the aqueous phase, over a pH range that encompasses the *pK*<sub>a</sub> of the drug. An approximate 1 mM solution of each substrate at a constant ionic strength of 0.167 M NaCl was titrated from low to high pH. The acid used was 0.5 N HCl and the base used was 0.5 N NaOH. The acid and base were standardized to four decimal places using NIST traceable standards. At the completion of the first titration, 1-octanol (HPLC grade), which was obtained from the Aldrich Chemical Co. and was water-saturated, was added, and the reverse titration was performed, returning the two-phase solution to the starting pH. The log *P* was determined by comparing the aqueous *pK*<sub>a</sub> to the *pK*<sub>a</sub> obtained with 1-octanol.

**RP-HPLC Lipophilicity Determinations.** HPLC analysis of the fluoroadamantane acids was performed on a Spectra-Physics HPLC system equipped with a P4000 quaternary pump and a AS3000 autosampler using a 4.6 × 150 mm Supelcosil LC-ABZ column (5 μm diameter) kept at ambient temperature, with a flow rate of 1.0 mL/

(34) Abraham, M. H., personal communication. We thank Professor Abraham for useful comments and an analysis of our log *P* data.

(35) Avdeef, A.; Comer, J. E. A.; Thomson, S. J. *Anal. Chem.* **1993**, *65*, 42–49.

min. An Applied Biosystems programmable UV detector was used for detection at 202 nm. Ratios of MeOH:0.1% TFA in water ranging from 45:55 to 65:35 were used as mobile phases, with 5% increments. The order of elution was also confirmed, using the 55:45 mobile phase mixture, by identifying each peak on a HP1100 system equipped with a Navigator LC/MS benchtop detector. No crossover of the order of elution was observed, under any of these conditions, for any of the compounds.

**Dipole Moment Calculations.** The computations were performed on a Silicon Graphics Indigo-2 workstation using a R4400 200-MHz processor. All computations were performed using the Merck Molecular Force Field,<sup>36</sup> the semiempirical Austin Model 1<sup>37</sup> or the ab initio Hartree–Fock level of theory as implemented in the Spartan software package, version 5.1.<sup>38</sup> A geometry optimization was performed at each level of theory, followed by a gas-phase computation of the dipole moments.

---

(36) Halgren, T. A. *J. Comput. Chem.* **1996**, *17*, 490–519 and following papers in the same issue.

(37) Dewar, M. J.; Zoebisch, E. G.; Healy, E. F.; Stewart, J. J. P. *J. Am. Chem. Soc.* **1985**, *107*, 3902–3909.

(38) SPARTAN software package, version 5.1, Wavefunction, Inc.: Irvine, CA.

**Acknowledgment.** The authors gratefully acknowledge insightful comments by Professor Jack Dunitz and stimulating discussions with Professor Dan Kemp and Drs. James Blake, Beryl Dominy, Edward Kleinman, and Jotham Coe. NMR support was provided by Dr. Walter Massefski and Diane Rescek. X-ray crystallographic results were obtained by Debra DeCosta. Log *P* and p*K*<sub>a</sub> determinations were determined by Dr. Cynthia M. Berger of pIon of Cambridge, Massachusetts. The authors would like to thank Dr. Amy Antipas and Ms. Barbara J. Brockhurst for their help with the LC-MS analysis.

**Supporting Information Available:** Experimental details and spectral data for all new compounds, crystal and refinement parameters and tables of atomic coordinates, equivalent isotropic displacement coefficients, bond lengths, bond angles, anisotropic displacement coefficients, and H-atom coordinates and isotropic displacement coefficients for fluoradamantane carboxylic acids **1**, **3**, and **7** (PDF). This material is available free of charge via the Internet at <http://pubs.acs.org>.

JA992652X